Controllers for Quadratic Stability and Performance of a Benchmark Problem

I.E. Kose, F. Jabbari, W.E. Schmitendorf, J.N. Yang
School of Engineering
University of California
Irvine, CA 92697

ABSTRACT: Recently developed quadratic stability and performance control techniques are used to design controllers for the active mass driver (AMD) benchmark problem. Several designs are obtained and analyzed to highlight the utility of the proposed technique. Solution through the use of linear matrix inequalities is presented and extensions to systems with modeling error, actuator/sensor malfunction and saturating controllers are discussed. Simulation results indicate that the performance of the control techniques is quite remarkable.

1 Introduction

In this paper, we apply the quadratic stability and performance technique to design dynamic (full order) output feedback control laws. In the simplest form, this approach coincides with the standard H_∞ method, which has been used in a variety of civil engineering applications (see references [9,13,18,19] or reference [7] for use in μ-synthesis, among others). The connections between the quadratic stability framework and the H_∞ techniques were discussed, among many, in references [24,8,12]. The quadratic stability framework used here, can be extended to address a variety of important considerations that are faced in full scale implementations of active control technologies.

While there have been some experimental verifications[23], a comprehensive evaluation of the proposed control laws have not been available. The purpose of this paper is to develop controllers for the Active Mass Driver (AMD) benchmark problem[22], with its associated constraints (e.g., magnitude of input) and suggested input records. The performance of the controllers developed is demonstrated by the simulation results.

The benchmark problem provides several important challenges that are faced in large scale implementations, including limits on the order of the compensator, the associated model reduction and the resulting errors, digital implementation, sensors noise, actuator dynamic, etc. Other issues, such as hardware reliability and actuator saturation for large earthquake episodes, are among the remaining critical issues. The basic framework presented here can

be used to address a variety of these critical issues, in a straightforward fashion. Such extensions are briefly discussed in Section 2, along with a variety of preliminary and background materials. In Section 3, detailed designs of the controllers are illustrated through numerical simulations for the benchmark problem. The performance of the proposed controllers for the AMD benchmark problem is also demonstrated in Section 3.

2 Preliminaries and Background

In this section, the basic notations and preliminary materials are presented, along with the main approach used. The equations (inequalities) used in the construction of the controller and the related main issues are listed, and some discussion on the extension to more difficult cases is also provided. Simulation results and the related discussions are presented in the next section.

2.1 Notation

Consider the design model used in Spencer, et al. (1997)

$$\begin{cases} \dot{x}_r(t) &= A_r x_r(t) + B_r u(t) + E_r \ddot{x}_g \\ z_r(t) &= C_{zr} x_r(t) + D_{zr} u(t) + F_{zr} \ddot{x}_g \\ y_r(t) &= C_{yr} x_r(t) + D_{yr} u(t) + F_{yr} \ddot{x}_g + \mathrm{v}_r \end{cases} \tag{1}$$

where x_r is the state of the reduced order system (i.e., design model), y_r is the measurement output vector, and z_r is the controlled output vector containing regulated response; e.g., displacements, velocities and accelerations of the floors and actuator, as discussed in reference [22]. Matrices C_{yr}, and C_{zr} relate the measured and regulated responses to the reduced-order (10 states) state variables that are not physical quantities.

For clarity and to be consistent with the notations used in the robust control literature, we use the standard state space representation of the form

$$\begin{cases} \dot{x}(t) &= Ax(t) + B_1 w(t) + B_2 u(t) \\ z(t) &= C_1 x(t) + D_{11} w(t) + D_{12} u(t) \\ y(t) &= C_2 x(t) + D_{21} w(t) + D_{22} u(t) \end{cases} \tag{2}$$

The two representations above are interchangeable. Clearly, $x(t) = x_r(t)$, $z(t) = z_r(t)$, $y(t) = y_r(t)$, $A = A_r$, $B_2 = B_r$, $D_{12} = D_{zr}$, $D_{22} = D_{yr}$, $C_1 = C_{zr}$, and $C_2 = C_{yr}$. However, the disturbance vector w of (2) contains both sensor noise and external disturbances (e.g., strong wind gust or ground acceleration). Therefore $w = [\ddot{x}_g \; v^T]^T$, $B_1 = [E_r \; 0]$, $D_{11} = [D_{zr} \; 0]$, and $D_{21} = [F_{yr} \; I]$.

The basic approach is to obtain a full order compensator of the form

$$\begin{cases} \dot{x}_c &= A_c x_c + B_c y \\ u &= C_c x_c + D_c y \end{cases} \tag{3}$$

such that the closed-loop system has desirable stability and performance characteristics. The standard approach is to assume that $D_{22} = 0$. Since in the benchmark problem a nonzero value for this matrix is identified, a simple transformation of the form

$$\bar{y} = y - D_{22}u$$

yields the following representation for the entire system (including compensator)

$$\begin{cases} \dot{x}(t) &= Ax(t) + B_1 w(t) + B_2 u(t) \\ z(t) &= C_1 x(t) + D_{11} w(t) + D_{12} u(t) \\ \bar{y}(t) &= C_2 x(t) + D_{21} w(t) \end{cases} \tag{4}$$

$$\begin{cases} \dot{x}_c &= \bar{A}_c x_c + \bar{B}_c \bar{y} \\ u &= \bar{C}_c x_c + \bar{D}_c \bar{y} \end{cases} \tag{5}$$

where

$$\bar{A}_c = A_c + B_c D_{22}(I - D_c D_{22})^{-1} C_c$$

$$\bar{B}_c = B_c + B_c D_{22}(I - D_c D_{22})^{-1} D_c$$

$$\bar{C}_c = (I - D_c D_{22})^{-1} C_c, \quad \bar{D}_c = (I - D_c D_{22})^{-1} D_c.$$

Equations (4) and (5) are of the form that will be used in the algorithms presented herein. Once $\bar{A}_c$, $\bar{B}_c$, $\bar{C}_c$ and $\bar{D}_c$ are calculated according to the procedures to be described below (and summarized in Section 2.4), A_c, B_c, C_c and D_c can be obtained via the the following

$$\begin{cases} D_c &= \bar{D}_c (I + D_{22} \bar{D}_C)^{-1} \\ C_c &= (I - D_C D_{22}) \bar{C}_c \\ B_c &= \bar{B}_c [I + D_{22}(I - D_c D_{22})^{-1} D_c]^{-1} \\ A_c &= \bar{A}_c - B_c D_{22}(I - D_c D_{22})^{-1} C_c \ . \end{cases} \tag{6}$$

After these matrices are obtained, they can be discretized and implemented according to the procedures outlined in reference [22]. In many instances the compensator in (5) can be assumed to be strictly proper (i.e., $\bar{D}_c = 0$) without any loss of generality. With such an assumption, equation (6) simplifies to $D_c = \bar{D}_c = 0$, $B_c = \bar{B}_c$, $C_c = \bar{C}_c = C_c$ and $A_c = \bar{A}_c - B_c D_{22} C_c$.

Finally, for a symmetric matrix X, the notation $X > 0$ ($X < 0$) means that X is a positive (negative) definite matrix, which is equivalent to the statement that all of the eigenvalues of X are strictly positive (negative). We can now discuss the basic approach and the algorithm used to obtain the compensator.

2.2 The Basic Technique

The basic approach used here is the quadratic stability with performance framework. For performance, we use guaranteed bounds on the induced L_2 norm of the appropriate transfer function. Throughout this paper, instead of the 'induced L_2 norm', we use the equivalent phrase of 'L_2 gain' of the system (since such a definition can also be applied in the presence of time variations and nonlinearities). Using (4) and (5) for the system and the compensator, the following closed-loop system is obtained

$$\begin{cases} \dot{x}_{cl} &= A_{cl}x_{cl} + B_{cl}w \\ z &= C_{cl}x_{cl} + D_{cl}w \end{cases} \tag{7}$$

where x_{cl} is the state vector of the closed-loop system (the states of the design model plus the compensator states)

$$x_{cl} = \begin{pmatrix} x \\ x_c \end{pmatrix} \; ; \quad A_{cl} = \begin{pmatrix} A + B_2\bar{D}_cC_2 & B_2\bar{C}_c \\ \bar{B}_cC_2 & \bar{A}_c \end{pmatrix} \; ; \quad B_{cl} = \begin{pmatrix} B_1 + B_2\bar{D}_cD_{21} \\ \bar{B}_cD_{21} \end{pmatrix}$$

and

$$C_{cl} = (C_1 + D_{12}\bar{D}_cC_2 \quad D_{12}\bar{C}_c) \; , \; D_{cl} = D_{11} + D_{12}\bar{D}_cD_{21}.$$

The main goal is to determine the compensator matrices $\bar{A}_c$, $\bar{B}_c$, $\bar{C}_c$, and $\bar{D}_c$ so that the closed-loop system has desirable stability and performance characteristics. Consistent with the definitions used in references [11,24], we use the following definition for stability and performance:

Definition 1: The system in (7) is said to be *quadratically stable with L_2 gain (or energy attenuation) of γ* if $R_{cl} = (\gamma^2 I - D_{cl}^T D_{cl}) > 0$ and there exists a constant positive definite matrix $\hat{P}$ such that

$$\hat{P}A_{cl} + A_{cl}^T\hat{P} + C_{cl}^TC_{cl} + [\hat{P}B_{cl} + C_{cl}^TD_c]R_{cl}^{-1}[\hat{P}B_{cl} + C_{cl}^TD_c]^T < 0. \tag{8}$$

Through the use of Lyapunov theory (with $x_{cl}^TPx_{cl}$ as the Lyapunov function), it is straightforward to show that if the system in (7) is quadratically stable (i.e., satisfies Definition 1) with L_2 gain (or energy attenuation) of γ, it is uniformly asymptotically stable and has L_2 (or energy) gain - from w to z - of less than γ. By L_2 gain, it is meant that $\|z\|_{L_2} < \gamma\|w\|_{L_2}$, where $\|z\|_{L_2}^2 = \int_0^\infty z^T(t)\,z(t)\,dt$. Thus, γ is used as a measure of how the

disturbance w influences entries in the controlled output z (e.g., interstory drifts). The objective of the control design is to minimize this influence by reducing the value of γ for the closed-loop system.

Through the use of Schur complement formula[4], equation (8) is equivalent to existence of a positive definite P such that

$$\begin{pmatrix} PA_{cl} + A_{cl}^T P & PB_{cl} & C_{cl}^T \\ B_{cl}^T P & -\gamma I & D_{cl}^T \\ C_{cl} & D_{cl} & -\gamma I \end{pmatrix} < 0 \, . \tag{9}$$

Consequently, the control design is reduced to finding a positive definite matrix P and a set of compensator matrices ($\bar{A}_c$, $\bar{B}_c$, $\bar{C}_c$, and $\bar{D}_c$) such that the inequality in (9) holds. If successful, the closed-loop system will be stable with a guaranteed L_2 gain (or energy attenuation) of less than γ. The smallest γ for which (9) is satisfied will be denoted as the minimum disturbance attenuation level, γ_{min}. Unfortunately, the unknown variables (i.e., P and the compensator matrices) enter (9) nonlinearly (e.g., product of P and $\bar{A}_c$). Solving for these unknowns, from (9), is a very difficult problem. Hence, the transformation of this problem into a simpler and solvable formulation is presented in the next section.

2.3 Solution via LMIs

As mentioned earlier, the control design requires finding the appropriate compensator matrices (i.e, $\bar{A}_c$, $\bar{B}_c$, $\bar{C}_c$ and $\bar{D}_c$) in (5) and a positive definite matrix P such that (9) holds. In the form presented in (9), the search for these matrices is difficult, due to the fact that the unknown variables enter the inequality in a nonlinear fashion. It is well known[3,8], however, the problem can be reformulated into a form that breaks the search for the unknown variables into two steps. In each of these steps, the unknown variables appear linearly and, as a result, the search for these variables becomes a convex search for which a variety of powerful numerical techniques are available. In the first step, a set of linear inequalities is obtained from which the matrix P can be calculated, but do not contain the compensator matrices explicitly. Once this step is completed, the second step involves another convex search, this time for finding the compensator matrices ($\bar{A}_c$, $\bar{B}_c$, $\bar{C}_c$, and $\bar{D}_c$). The following is a brief summary of the main steps in obtaining the compensator matrices.

The existences of a positive definite matrix P and compensator matrices, such that (9) holds, is equivalent to the existence of a pair of positive definite matrices $X > 0$, and $Y > 0$ such that the following three linear matrix inequalities (LMIs) hold *simultaneously*[3,8]

$$B_\perp^T \begin{pmatrix} AX + XA^T & XC_1^T & B_1 \\ C_1X & -\gamma I & D_{11} \\ B_1^T & D_{11}^T & -\gamma I \end{pmatrix} B_\perp < 0 \tag{10}$$

$$C_\perp \begin{pmatrix} YA + A^TY & YB_1 & C_1^T \\ B_1^TY & -\gamma I & D_{11}^T \\ C_1 & D_{11} & -\gamma I \end{pmatrix} C_\perp^T < 0 \tag{11}$$

$$\begin{pmatrix} X & I \\ I & Y \end{pmatrix} > 0 \tag{12}$$

in which A, B_1, C_1 and D_{11} are given in (2) and

$$B = [B_2^T \quad D_{12}^T \quad 0]^T, \quad , C = [C_2 \quad D_{21} \quad 0]. \tag{13}$$

In (10) and (11), the subscript '$\perp$' denotes a maximum rank matrix that spans the null space of the transpose of a matrix. In other words, matrix $B_\perp$ is any matrix such that the matrix $[B \quad B_\perp]$ is square and invertible and $B^TB_\perp = 0$. In general, $B_\perp$ can be constructed by using the singular value decomposition. Many software packages (e.g., MATLAB LMI toolbox) are available to calculate such matrices. More details regarding the properties of such matrices can be obtained from many references[3,4,6].

The first step, i.e., the search for X and Y in (10)-(12), is a convex search since the unknown variables enter the inequalities linearly (affinely). A variety of techniques are available for solving this problem, but the interior point techniques that were recently developed have been gaining wide-spread acceptance as a fast, accurate and efficient approach. The numerical results presented in this paper were all obtained with the MATLAB LMI toolbox[6]. Note that the compensator matrices do not appear in these inequalities explicitly (they will be calculated in the second step). Also, note that the three LMIs have to be solved simultaneously, due to the coupling condition in (12). This last feature is somewhat different from the H_2 problem, for example, where the separation principle allows sequentially solving the full state and observer equations.

The guaranteed L_2 gain (i.e., γ) appears linearly in equations (10)-(12). As a result, γ can be either set to a predetermined level, or minimized simultaneously with finding feasible X and Y (i.e., find the minimum value of γ for which (10)-(12) are feasible). Once γ_{min} is known, the search for the corresponding X and Y is guaranteed to result in appropriate matrices for any $\gamma \geq \gamma_{min}$. In most of the simulation results presented in Section 3, γ is

minimized in the search for X and Y. After matrices X and Y that satisfy (10)-(12) are calculated, we construct a feasible P for (9) according to

$$S = X - Y^{-1} \tag{14}$$

and

$$P = \begin{pmatrix} Y & -Y \\ -Y & S^{-1} + Y \end{pmatrix}. \tag{15}$$

Once this P is known, the remaining variables (i.e., the compensator matrices $\bar{A}_c$, $\bar{B}_c$, $\bar{C}_c$, and $\bar{D}_c$) in (9) appear linearly; i.e., (9) is now a linear matrix inequality in these remaining unknown variables. Hence, the second step is to use (9) to determine the unknown matrices $\bar{A}_c$, $\bar{B}_c$, $\bar{C}_c$, and $\bar{D}_c$, which is another convex search. The unknown matrices can be solved similar to the search for X and Y in (10)-(12) (e.g., through MATLAB LMI toolbox).

The lowest feasible value of γ, denoted by γ_{min}, can be found in the first step; i.e., searching for X and Y, as mentioned earlier. In the second step; i.e., searching for the compensator matrices, any value equal to or larger than γ_{min} can be used. In our simulation studies, instead of γ_{min}, we use $\gamma = \gamma_{min} + \epsilon$ in the second step, to reduce the potential numerical problems.

2.4 Control Design Algorithm

The algorithm for obtaining the control law presented above can be summarized as follows

(i) Choose an initial controlled output z with appropriate weightings on critical quantities (e.g., interstory drifts)

(ii) Obtain the corresponding C_1, D_{11} and D_{22}, by using the appropriate rows of C_{zr}, D_{zr} and F_{zr}

(iii) Use (10)-(12) to obtain X, Y and the minimum value of γ, X.

(iv) Construct the P matrix according to (14)-(15)

(v) Use (9) to search for $\bar{A}_c$, $\bar{B}_c$, $\bar{C}_c$, $\bar{D}_c$, using P obtained in step (iv) and any $\gamma \geq \gamma_{min}$

(vi) Obtain A_c, B_c, C_c, D_c from (6)

(vii) Discretize and implement A_c, B_c, C_c, D_c, according to reference [22]

Steps (i) and (ii) require extraction of appropriate rows (and possibly multiplying some rows by scaling constants) from the data provided for the benchmark problem (see (2) and (1) and the related discussion). Steps (iv), (vi) and (vii) involve routine matrix manipulations. Steps (iii) and (v) constitute the two convex searches that were discussed earlier. All the simulation results shown in Section 3 are obtained through the use of MATLAB's LMI-toolbox. The dimension of matrixes X and Y is the same as the state matrix A (i.e., 10×10 in the benchmark problem). The dimension of the compensator matrix A_c is also the same as A since the procedure discussed here concerns the design of full order output feedback control laws. The dimension of the rest of the compensator matrices is related to the number of actuators and sensors used. Finally, an alternative approach in Step (iii) would be not to minimize γ and set γ to any value larger than the minimum obtainable (i.e., step (iii) would use (10)-(12) to obtain X, Y for some γ).

As discussed further below, the framework presented here can be used to address a variety of critical issues (e.g., hardware reliability/malfunction and saturation) simultaneously. However, if no other considerations are taken into account (i.e., there is no uncertainty, no multi-objective, no saturation), then the approach used here is equivalent to the basic H_∞ technique. For example, satisfaction of the quadratic stability with L_2 gain of γ is equivalent to having an H_∞ norm of less than γ (for the transfer function from w to z; i.e., $C_{cl}[sI - A_{cl}]^{-1}B_{cl} + D_{cl}$). The optimal H_∞ solution corresponds to the minimum value of γ obtained from the the three LMIs in (10)-(12). For the simulation results presented in this paper, the basic quadratic stabilization (with performance) approach has been applied to the AMD benchmark problem.

2.5 Extensions

Only the basic quadratic stabilizability with performance problem has been presented in this paper, since we are concerned with the simulation studies for the performance of the AMD benchmark problem. A variety of other issues, however, can be anticipated in practical implementation that require careful considerations. In this subsection, we review three important extensions; (i) modeling error, (ii) actuator/sensor malfunction or unreliability, and (iii) actuator saturation.

2.5.1 Modeling Error

Due to inherent modeling errors involved in large civil engineering structures, the issue of robustness of the controller performance to modeling errors is a natural concern. With modeling errors, the approach presented above can be modified to obtain controllers that are guaranteed to perform at a desirable level (i.e., a given γ). The state feedback design can easily incorporate the modeling error and it involves a convex search (i.e., a search for two matrices that satisfy a set of LMIs similar to (10)). However, the output feedback problem is not in general convex and thus considerably harder to solve. With the framework presented above, it has been shown how the number and location of sensors can be chosen such that the problem can be make into two sequential convex problems[10]. Also, reference [15], discusses conditions under which observers can be obtained that recover the properties of a state feedback control law, for the case of norm bounded uncertainty. Similar results[10,11,15]can be used for the determination of type, number and location of sensors that simplifies the control design process, when significant modeling error is present.

2.5.2 Actuator/Sensor Malfunction

A critical issue in the implementation of active control systems is the possible malfunction failure) of hardware, such as actuators or sensors. Malfunction (or failure) of actuators or sensors can be expressed in terms of the gain deviations (or variations) that can be quite large during the start-up period. These variations could come from power fluctuations, non-linearities, partial actuator failure or any type of variation that causes time varying gain changes in the sensor or actuator signals.

Malfunction of actuators described above has been incorporated into the quadratic stability framework[2],and it is founds that there is a natural tradeoff between performance and the bounds on the malfunction or reliability. In principle, the gain deviation due to the malfunction of actuators or sensors can be considered as modeling error (or robustness) problem, hence it can be taken into account in the formulation described in Section 2.5.1 However, because of the specific nature of the actuator malfunction, we have obtained stronger results. Among these are lower computational costs and the convexity of the search process for controllers with a specific structure[1,2].

2.5.3 Saturating Actuators

Another important issue is the actuator saturation. Due to the limited capacity of an actuator, as well as the random nature of earthquake excitations, actuators may become saturated, particularly under near-field earthquakes. Although one can design a controller that will not saturate under the maximum credible earthquake, the resulting controller will have a low gain matrix leading to a poor control performance for the design earthquake. Since civil engineering structures are designed to be stable without control, most of the control methodologies in the literature which are geared to stabilizing systems with actuator saturation are of little use. Thus a controller that maintains its high performance under unexpectedly strong earthquakes, by utilizing its full capacity is highly desirable.

The issue of actuator saturation can be incorporated in the quadratic stability framework used here[16,17]. This is accomplished by creating a multi-objective problem, to provide a desirable performance (i.e., L_2 gain) as well as using estimates for the ellipsoid of reachability. The resulting problem will form a convex search for the state feedback problem, which under mind assumptions (particularly for earthquake applications) is guaranteed to work with a simple observer-based output feedback controller. As shown in references [16] and [17], the multi-objective approach can be used to solve a problem that has the following features: (i) it guarantees substantial improvement in performance, (ii) the level of performance is explicitly related to the actuator saturation levels and the peak ground acceleration of the design earthquake, and (iii) it operates at, or close to, peak actuator capacity.

3 Simulation Results

Before discussing the details of the simulation results, a few issues will be reviewed:

Strictly Proper vs. Proper Controller

In general, the approach outlined above yields a proper controller (i.e., $\bar{D}_c$ is not typically zero). However, as shown in reference [14], when the size of D_{11} is small (as is the case in the benchmark problem), this feedthrough term can be set to zero without any loss of generality. Furthermore, in the last step of the design (i.e., the LMIs to obtain the compensator matrices), matrix $\bar{D}_c$ can be set to be zero (the search becomes that of finding three matrices $\bar{A}_c$, $\bar{B}_c$ and $\bar{C}_c$ such that (9) is satisfied). Such a compensator does not have a direct feed from measurements to the control input, and thus reduces the effects of sensor

Table 1: Peak Actuator Values for

$z = [x_1\ x_2\ x_3\ x_m\ \dot{x}_1\ \dot{x}_2\ \dot{x}_3\ \dot{x}_m\ \ddot{x}_1\ \ddot{x}_2\ \ddot{x}_3\ \ddot{x}_m]^T$

Case	γ	max(u) Volts	max(x_m) cm	max($\ddot{x}_m$) g
A.1	25	3.4395	11.1218	39.3446
A.2	50	1.5145	5.4829	8.6906
A.3	100	1.45020	5.2560	7.8655

noise and simplifies the implementation step.

When this structure (i.e., $\bar{D}_c = 0$) is not explicitly enforced, the approach used here results in nonzero $\bar{D}_c$ which has entries that are several orders of magnitude smaller than the rest of the compensator matrices. Keeping the same control output, z, and performance bound, γ, an interchange of proper and strictly proper compensators results in no noticeable changes in any of the measured quantities.

Number of Measurements

All simulation results presented for the dynamic output feedback use the same output measurements as in reference [22]; i.e.,

$$y = [\ddot{x}_1 \quad \ddot{x}_2 \quad \ddot{x}_3 \quad \ddot{x}_m\ ]^T .$$

No discernible difference was observed when different combination of sensors were used (as low as 2 sensors or as many as 6 - including the ground acceleration). By keeping the sensors the same as in reference [22], comparisons become somewhat easier.

Ground Acceleration and Recovery of Full State Performance

The fact that using the ground acceleration measurement did not improve the controller performance is not surprising. Due to the relatively small size of D_{11}, such a measurement does not improve the performance of state feedback controllers (i.e., the full information case is not better than the state feedback case). As a result, the low impact of ground acceleration measurement was to be expected.

Simulation Results

The first step in the design is to choose an appropriate controlled output (i.e. z). Typically, a combination of undesirable quantities are incorporated in z (e.g., interstory drifts or

floor accelerations). For simplicity, we first use the vector z as defined in reference [22] as the control output; i.e.,

$$z^T = [x_1\ x_2\ x_3\ x_m\ \dot{x}_1\ \dot{x}_2\ \dot{x}_3\ \dot{x}_m\ \ddot{x}_1\ \ddot{x}_2\ \ddot{x}_3\ \ddot{x}_m].$$

Recall that this vector has all relative displacements, their derivatives, floor absolute accelerations, the displacement, velocity and the acceleration of the actuator mass as its entries.

With the controlled output z above, the open-loop $\gamma_{min} = 274.89$ is determined from (10)-(12) by setting $B_2 = 0$ and $D_{12} = 0$ (see step (iii) of the procedure in Section 2.4). For the closed-loop system ($B_2 \neq 0$, $D_{12} \neq 0$), the minimum γ is obtained from (10)-(12) as $\gamma_{min} = 24.04$. The next step, step (iv), is to use $\gamma = \gamma_{min} + 1 = 25$ in (9) along with P obtained in step (iii) to determine the compensator matrices. After the controller is designed, the peak response quantities of the evaluation model[22] are computed using the El Centro earthquake input. Some results are shown in the first row of Table 1, denoted by Case A.1. In Table 1, the peak control command, peak AMD mass displacement and peak AMD mass acceleration are denoted by $max(u)$, $max(x_m)$, and $max(\ddot{x}_m)$, respectively. In reference [22], all three of these quantities are required to be constrained within certain limits. The results in Table 1 for Case A.1 indicate that all three violate the constraints. As a result, it is necessary to modulate the control effort and response quantities so that all of the constraints are satisfied.

In the present formulation, there are two possible approaches to modulate the control efforts vs the structural response. One approach is to manipulate the value of γ used and the other is to alter the controlled output z. Note that the quantities shown in Table 1 are associated with the control effort, since $max(x_m)$ and $max(\ddot{x}_m)$ are related to the control command u. Now, we consider the first approach by keeping the same z as before but increasing the value of γ above the minimum of 24.04 (since an increase in γ will reduce the control effort or increase the structural response). Hence, values of $\gamma = 50$ and 100 are used in the procedure in Section 2.4 to determine the compensator matrices (For these cases, γ is not minimized and it is set to 50 and 100, respectively, in both steps (iii) and (v)). Such controllers are denoted by Cases A.2 and A.3, respectively. Under El Centro earthquake, the peak response quantities of the evaluation model for the cases A.2 and A.3 are shown in Table 1. As observed from Table 1, increasing γ leads to a very limited success, since the constraints are still violated. Even if γ is increased to 200, the constraint on $\ddot{x}_m$ is still violated.

Table 2: Controlled Outputs and Minimum L_2 Gains

Case	Controlled Output	Open-loop γ_{min}	Closed-loop γ_{min}	Ratio
A	$z = [x_1\ x_2\ x_3\ x_m\ \dot{x}_1\ \dot{x}_2\ \dot{x}_3\ \dot{x}_m\ \ddot{x}_1\ \ddot{x}_2\ \ddot{x}_3\ \ddot{x}_m]^T$	271.89	24.04	0.088
B	$z = [x_1\ x_2\ x_3\ 5x_m\ \dot{x}_1\ \dot{x}_2\ \dot{x}_3\ 5\dot{x}_m\ 3\ddot{x}_1\ \ddot{x}_2\ \ddot{x}_3\ 10\ddot{x}_m]^T$	437.53	113.15	0.257
C	$z = [x_1\ x_2\ x_3\ x_m\ \dot{x}_1\ \dot{x}_2\ \dot{x}_3\ \dot{x}_m\ \ddot{x}_1\ \ddot{x}_2\ \ddot{x}_3\ 20\ddot{x}_m\ 3u]^T$	502.77	72.69	0.145
D	$z^T = [x_1\ x_2\ x_3\ \dot{x}_1\ \dot{x}_2\ \dot{x}_3\ \dot{x}_m\ \ddot{x}_1\ \ddot{x}_2\ \ddot{x}_3\ 17\ddot{x}_m\ ]$	348.93	59.40	0.170

Consequently, we shall consider the second approach in which the controlled output z is changed. Here, different z vectors will be used, referred to as Cases B-D in Table 2. For a given z, the P matrix and γ_{min} are determined from (10)-(12), as in Step (iii). Then, the controller is obtained from (9) with the P matrix obtained above and $\gamma = \gamma_{min} + 1$, as in step (v). In Table 2, different cases correspond to different weighting used for the controlled output z (from adding u to z, to heavily penalizing the acceleration and the displacement of the AMD mass). The other entries in Table 2 show the γ_{min} for open-loop and closed-loop systems for each case. Note that the choice of z alters the open-loop γ_{min} as well as the closed-loop γ_{min}. The last column in Table 2 denotes the ratio of the closed-loop γ_{min} to the open-loop γ_{min}.

While more details will be provided below, throughout the simulations it was observed that the El Centro earthquake produced the larger peak actuator voltage, AMD mass displacement and acceleration. Hachinohe earthquake, however, resulted in values that were recorded in J6-J10 (since their corresponding values were always larger than those of the El Centro). Also, as the tables below indicate, the acceleration of the AMD mass was the critical constraint for these controllers.

Tables 3 and 4 present the results of simulations. Table 3 shows the performance indices J1-J5 and $\sigma(u)$, when the system is subjected to stochastic earthquake with $\zeta_g = 0.3$ and $w_g = 37.3$. Table 4 presents the performance indices J6-J10, and the peak values for actuator commands (in volts), displacement and acceleration of the AMD mass (in centimeters and g's respectively). This table corresponds to the El Centro and Hachinohe earthquake inputs. Table 4 indicates that the larger control command results in the smaller performance indices J6 and J7, as well as the larger values for indices J8-J10 as expected. As observed from Tables 3 and 4, the performance of the controllers, i.e., Cases B,C, and D, are quite remarkable.

As mentioned earlier, the acceleration of the AMD mass, $\ddot{x}_m$, is the most likely constraint

to be violated, and there is a strong correlation between u and $\ddot{x}_m$. Hence, it might be possible to improve the performance of the controller by making further modifications to z by considering the explicit relationship between u and $\ddot{x}_m$ and pushing both toward their allowable limits . However, considering the limit of $\ddot{x}_m$, the resulting improvements may be rather modest.

Figures 1-4 present a few representative frequency responses. For brevity, all figures correspond to the controller in Case C. Figure 1 shows the loop-gain transfer function, similar to Figure 6 of reference [22]. Figures 2-4 show the transfer function from the input (earthquake) to the first floor relative displacement (x_1), the displacement of the AMD mass (x_m) and the absolute acceleration of the AMD mass ($\ddot{x}_m$), respectively. In these plots, the dotted curves correspond to the open-loop response.

Note that the controller had primarily lowered the peaks of the response in Figure 2. In Figures 3 and 4, the controller has resulted in higher gains at the low and intermediate frequencies. This is not surprising since Figures 3 and 4 correspond to the motion of the AMD mass, and the relatively high gain of the control law is related to the increased motion for the AMD mass. Also, note that the controller has resulted more of an increase in the displacement response (Figure 3) than the acceleration response (Figure 4), due to the high weighting placed on the mass acceleration in Cases C (recall that this acceleration was often the critical constraint).

4 Conclusions

Quadratic stability and performance control techniques developed recently for the design of dynamic output feedback compensators have been presented and applied to the AMD benchmark problem. Solutions through the use of linear matrix inequalities have been obtained. Step by step design procedures for the controller have been described. Several controllers have been designed for the AMD benchmark problem to illustrate the utility of the proposed technique. Simulation results are presented so that the performance of the proposed control design technique can be evaluated. These results are indicative of the ability of the proposed method to significantly reduce interstory drifts and floor accelerations within the constraints of the benchmark problem.

Without other considerations, such as system uncertainty, multi-objective criteria, etc, the approach presented is equivalent to the basic H_∞ technique. However, the main advan-

Table 3: Performance Indices: Stochastic Earthquakes

Case	J_1	J_2	J_3	J_4	J_5	$\sigma(u)$
B	0.2156	0.3252	0.7264	0.7148	0.6636	0.2351
C	0.1781	0.2725	0.9380	0.9058	0.8106	0.3202
D	0.1678	0.2556	1.360	0.9710	0.8757	0.4664

Table 4: Performance Indices: El Centro and Hachinohe Earthquakes

Case	J_6	J_7	J_8	J_9	J_{10}	$\max(u)$	$\max(x_m)$	$\max(\ddot{x}_m)$
B	0.3861	0.6813	1.3203	1.2696	1.3519	0.9932	3.5853	4.612
C	0.3636	0.6318	2.1619	1.8235	1.4240	1.4033	4.9935	5.536
D	0.3547	0.6097	2.4823	2.1518	1.7039	1.5059	5.3850	5.849

tage of the proposed technique lies in its ability to account for other critical issues, including modeling errors, actuator/sensor malfunction, and controller saturation. Extension of the present formulation to cover these critical issues has been discussed briefly.

ACKNOWLEDGMENT: This research was supported by National Science Foundation Grants BCS-93-02101 and CMS-96-15731. The authors would like to thank Dr. J.C. Wu for his assistance in managing the simulation input information.

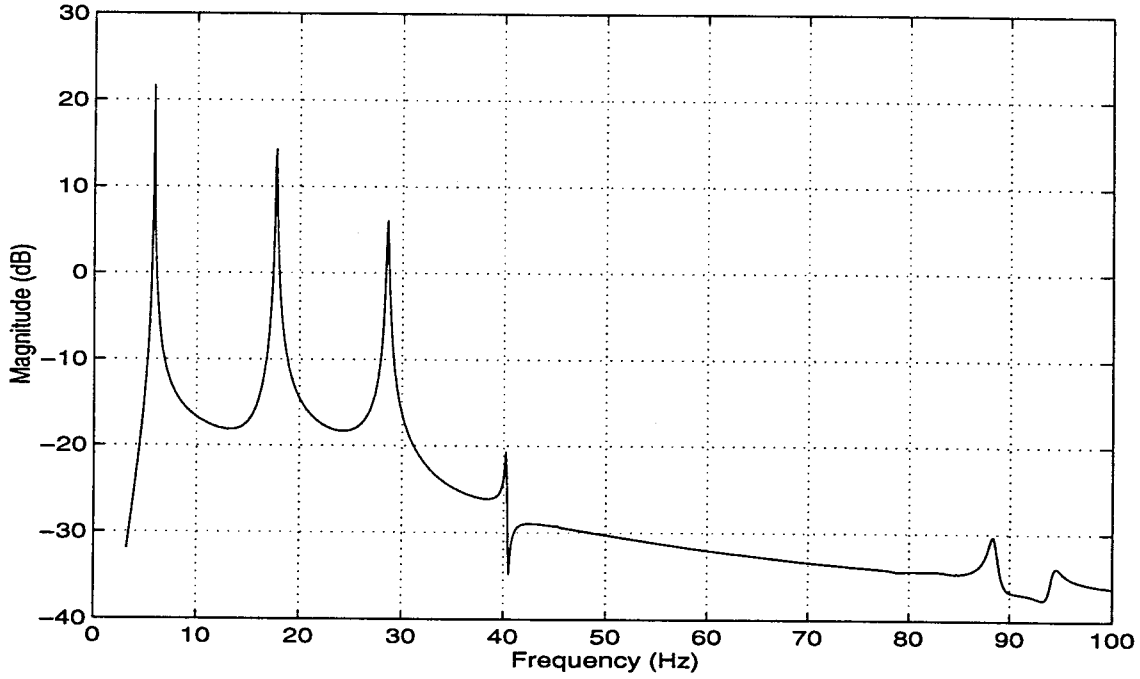

Figure 1: Loop-gain transfer function for Case C

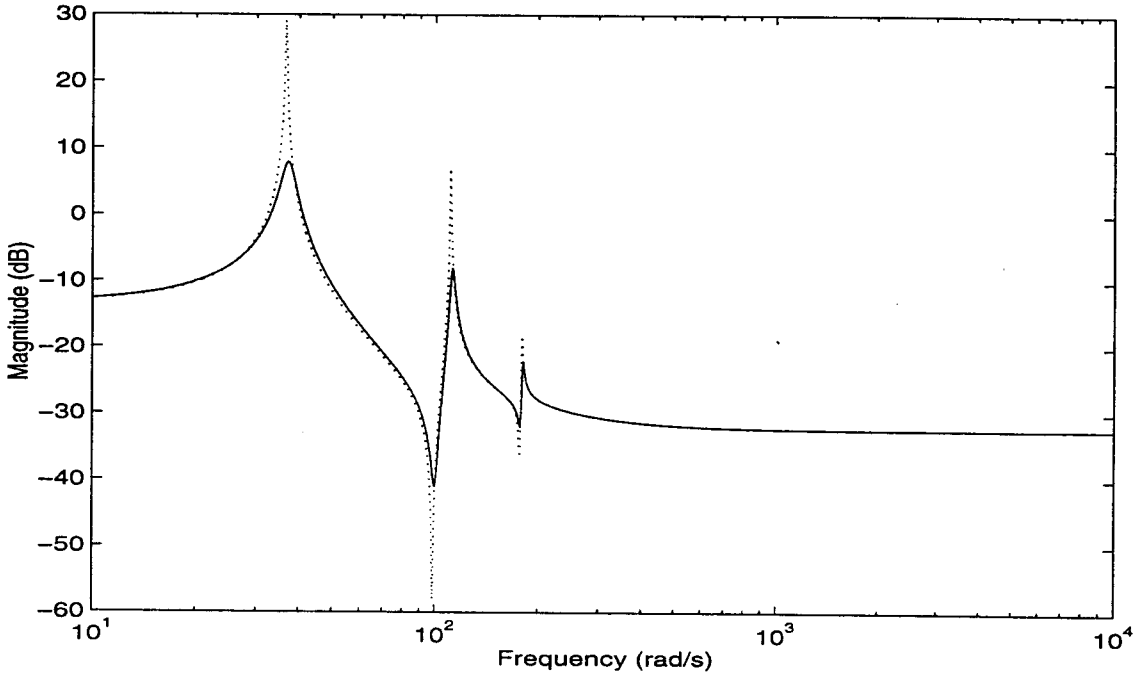

Figure 2: Transfer function from $\ddot{x}_g$ to x_1 for Case C

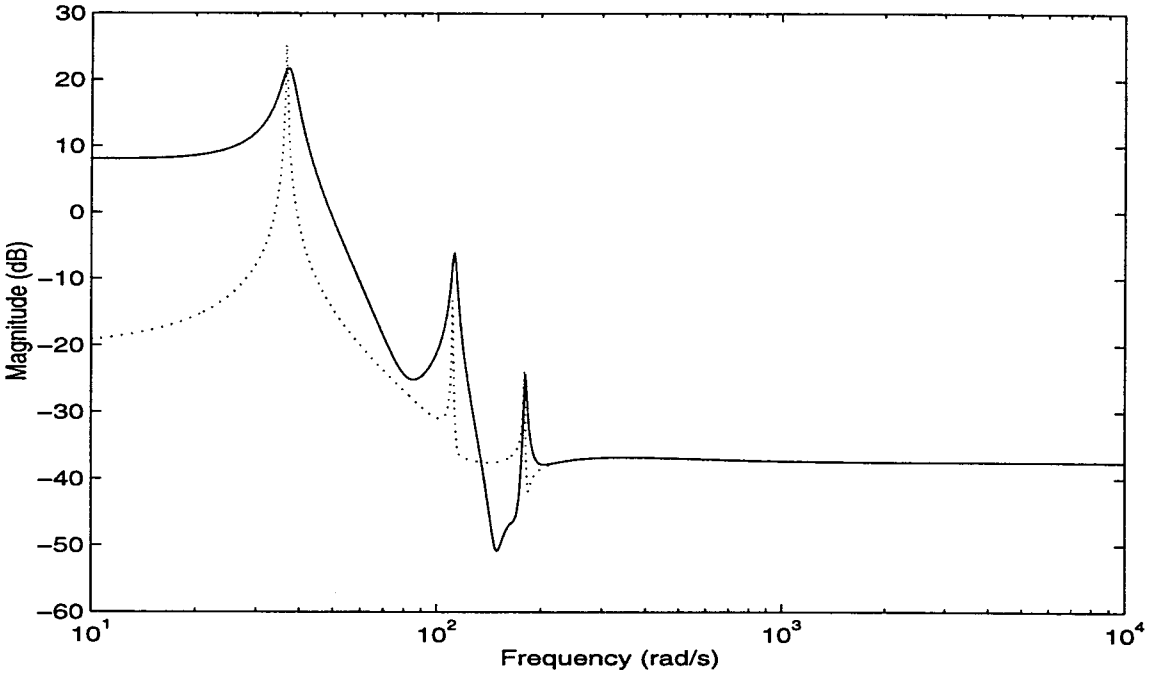

Figure 3: Transfer function from $\ddot{x}_g$ to x_m for Case C

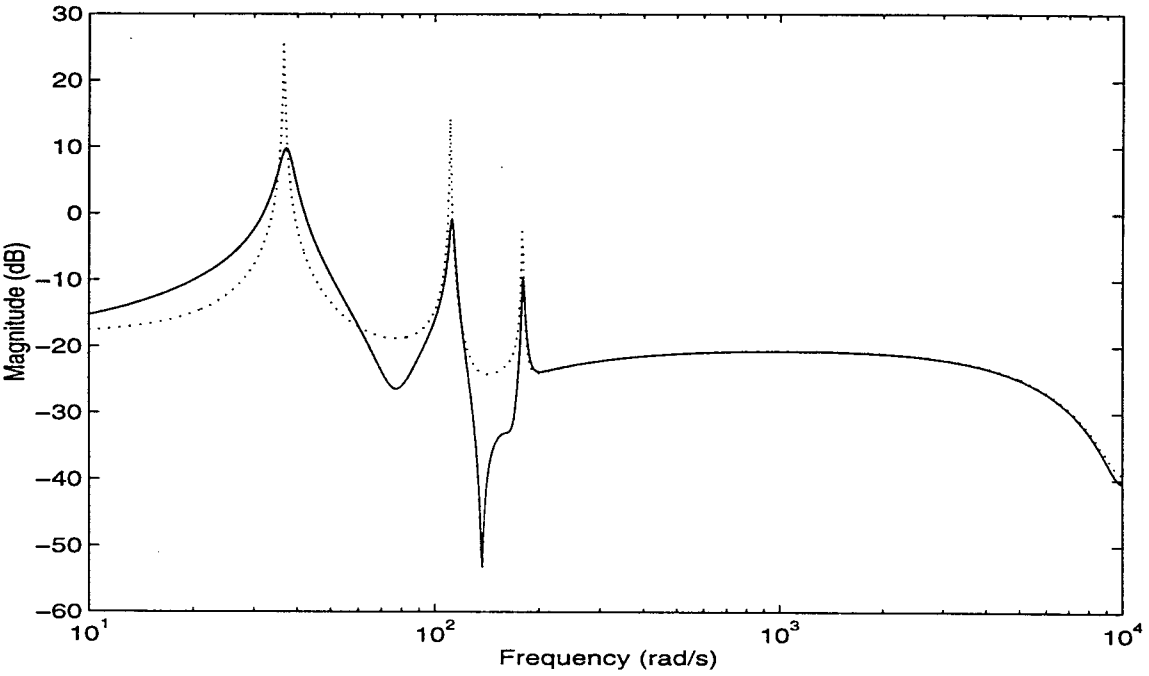

Figure 4: Transfer function from $\ddot{x}_g$ to $\ddot{x}_m$ for Case C

References

1. Alt, T.R., Jabbari, F., "A reliable control system design for smart structures," ASME International Congress, San Francisco, CA, November 1995.

2. Alt, T.R., Jabbari, F., Yang, J.N., "Reliable control design for buildings under seismic excitation," *Eleventh World Conference on Earthquake Engineering* (11WCEE), Elsevier Science, Ltd, Paper No. 1545, 1996.

3. Apkarian, P., Gahinet, P., "A linear matrix inequality approach to H_∞ control," *International Journal of Robust and Nonlinear Control*, Vol 4, pp 421-448, 1994.

4. Boyd, S., El Ghaoui, L., Feron, E., Balakrishnan, V., *Linear Matrix Inequalities in System and Control Theory*, SIAM Publishing, Philadelphia, PA, 1994.

5. Chilali, M., Gahinet, P., "H_∞ Design with Pole Placement Constraints: An LMI Approach", *IEEE Trans. on Auotmatic Control*, Vol 41, No 3, pp 358-367, 1996.

[6] Gahinet, P. , Nemirovski,, Laub., A.J., Chilali, M., *LMI Control Toolbox*, The MATHWORKS, Inc., 1995.

7. Hsu, C.C., Calise, A.J., Goodno, B.J., Craig, J.I., "Performance evaluation of robust controllers in earthquake structural dynamics problems," Proceedings of the American Control Conference, Seattle, Wa, pp. 1916-1920, 1995.

8. Iwasaki,T., Skelton, R., "All controllers for the general H_∞ control problem: LMI existence condition and state space formulas", *Automatica*, Vol 30, No 8, pp 1307-1317, 1994.

9. Jabbari, F., Schmitendorf W.E., and Yang, J.N., "H_∞ Control for seismic-excited building with acceleration feedback," *Journal of Engineering Mechanics, ASCE*, Vol 121, No. 9, pp 994-1002, 1995.

10. Jabbari, F., "Output Feedback Controllers for Systems with Structural Uncertainty," to appear in *IEEE Trans. on Automatic Control*, Vol 42, No 5, pp 715-719, 1997.

11. Jabbari, F., Kose, I.E., "Design of controllers for disturbance attenuation of uncertain systems," to appear in *ASME J. Dynamics, Control and Measurement*, 1997 (Also in Proceedings of ASME International Congress, 1995).

12. Khargonekar, P.P., Petersen, I.R., Zhou, K, "Robust Stabilization of Uncertain Linear Systems: Quadratic stabilization and H_∞ Control Theory'" *IEEE Transaction on Auotmatic Control*, Vol 35, pp 356-361, 1990.

13. Kose, I.E., Schmitendorf W.E., Jabbari, F. and Yang, J.N., "H_∞ Active seismic response control using static output feedback," *Journal of Engineering Mechanics, ASCE*, Vol 122, No 7, pp 651-659, 1996.

14. Kose, I.E., Jabbari, F., Schmitendorf, W.E., "A Direct Characterization of L_2 Gain Controllers for LPV systems," Preceddings 1996-CDC, pp 3990-3995, 1996.

15. Kose, I.E., Jabbari, F., "Disturbance Attenuation for Systems with Real Parametric Uncertainty," Proceedings of American Control Conference (ACC-97), Albuquerque, New Mexico, 1997.

16. Nguyen, T., Jabbari, F., "Disturbance Attenuation for Systems with Input Saturation: an LMI Approach," Proceedings of American Control Conference (ACC-97), Albuquerque, New Mexico, June 1997.

17. Nguyen, T., Jabbari, F., de Miguel, S. "High Performance Control of Buildings under Seismic Excitation: Designs for Saturating Actuators," Proceedings of Eleventh VPI&SU Symposium on Structural Dynamics and Control, Blacksburgh, Viginia, May 1997.

18. Schmitendorf, W.E., Marti, S. Jabbari, F., Yang, J.N., "Active control of seismically-excited buildings with model uncertainty," Proceedings of Fifth U.S. National Conference on Earthquake Engineering, Chicago, IL, pp 951-959, 1994.

19. Schmitendorf, W.E., Jabbari, F., Yang, J.N., "Robust Control Techniques for Buildings Under Earthquake Excitation," *Earthquake Engineering and Structural Dynamics*, Vol 23, pp 539- 552, 1994.

20. Schmitendorf, W.E., Jabbari, F., Yang, J.N., "An LMI Approach for Robussr Control Laws for Structures Under Environmental Excitation", Proceedings of IFAC-96, San Francisco, pp 181-186, 1996.

21. Skelton, R.E., Stoustrup, Iwasaki, T., "The H_∞ problem using static output feedback," *International Journal Robust and Nonlinear Control*, Vol 4, pp 449-455, 1993.

22. Spencer, B.F., Dyke, S.J., Deoskar, H.S., "Bencjmark Problems in Structural Control Part I: Active Mass Driver System," *Earthquake Engineering and Structural Dynamics*, January 1997.

23. Yang, J.N., Wu, J.C., Reinhorn, A.M., Riley, M., Schmitendorf W.E., and Jabbari, F., "Experimental verification of H_∞ and sliding mode control for seismically excited buildings," *Journal of Structural Engineering, ASCE*, vol 122, No 1, pp 69-75, 1996.

24. Zhou, K., Khargonekar, P.P., Stoustrup, J., Niemann, H.H., "Robust performance of systems with structured uncertainties in state space," *Automatica*, Vol 31, pp 249-255, 1995.